Supplementary information for

Translocation kinetics and structural dynamics of ribosomes are modulated by the conformational plasticity of downstream pseudoknots

Bo Wu [a], Haibo Zhang [b], Ruirui Sun [a], Sijia Peng [a], Barry S. Cooperman [b], Yale E. Goldman [c,*], Chunlai Chen [a,*]

[a,] *School of Life Sciences; Tsinghua-Peking Joint Center for Life Sciences; Beijing Advanced Innovation Center for Structural Biology, Tsinghua University, Beijing, China, 100084*
[b,] *Department of Chemistry, University of Pennsylvania, Philadelphia, PA 19104*
[c,] *Pennsylvania Muscle Institute, School of Medicine, University of Pennsylvania, Philadelphia, PA 19104*

**Correspondence: chunlai@mail.tsinghua.edu.cn (C.C.) and goldmany@mail.med.upenn.edu (Y.E.G.)*

Table S1 mRNA sequences and properties of mRNA structures

mRNA structure	-1 PRF efficiency measured in rabbit reticulocyte lysate (%)	ΔG (kcal/mol) (1,2)	Average unfolding force (pN)(2)	mRNA sequences with a common non-slippery sequence (from 5' to 3') [a]
PL	N.A.	-5.6	NA	GGGACCAGCAGGCGGACCACCGGACCAGGGAAGUCAAAAAUUUAAAA GUUAA AGGGAG AUAUA **AUG** UAU UUU GUU CGU *GAA UAU GAA UAU GAA UAU GAA UAU GAA UAU* UAA AAA AAA GAAUUC
PT2G32	2 (3)	-63	40	GGGACCAGCAGGCGGACCACCGGACCAGGGAAGUCAAAAAUUUAAAA GUUAA AGGGAG AUAUA **AUG** UAU UUU GUU CGU *CAC UGA CCA GCU AUG AGG UCA UAC AUC GUC AUA GCA C* UAA AAA AAA GAAUUC
PEMV1	9 (4)	-39	31	GGGACCAGCAGGCGGACCACCGGACCAGGGAAGUCAAAAAUUUAAAA GUUAA AGGGAG AUAUA **AUG** UAU UUU GUU CGU *UUA UUC CGG UCG ACU CCG GAG AAA CAA AGU CAA* UAA AAA AAA GAAUUC
ScYLV	15 (5)	-60	42	GGGACCAGCAGGCGGACCACCGGACCAGGGAAGUCAAAAAUUUAAAA GUUAA AGGGAG AUAUA **AUG** UAU UUU GUU CGU *CCA AGT GGC GCC GAC CAC TTA AAA ACA CCG GA* UAA AAA AAA GAAUUC
HERV	20 (3)	N.A.	52	GGGACCAGCAGGCGGACCACCGGACCAGGGAAGUCAAAAAUUUAAAA GUUAA AGGGAG AUAUA **AUG** UAU UUU GUU CGU *CAA AGG GGC CAG CCU CAG GCC CCA CAA CAA ACU GGG GCA U* UAA AAA AAA GAAUUC
VMV	28 (6)	N.A.	30	GGGACCAGCAGGCGGACCACCGGACCAGGGAAGUCAAAAAUUUAAAA GUUAA AGGGAG AUAUA **AUG** UAU UUU GUU CGU *AGG AGG GGG CCA CGU GUG GUG CCG UCC GCG CCC CCU AUG UUG UAA CAG AAG CAC CAC C* UAA AAA AAA GAAUUC
copA-WT	N.A.	N.A.	N.A.	GGGACCAGCAGGCGGACCACCGGACCAGGGAAGUCAAAAAUUUAAAA GUUAA AGGGAG AUAUA **AUG** UAU UUU GUU CGU *GAA CCG CTG GCG GAG TCA TCA ATC CCG TCG GAA GCA CTG ACA GCG GTT TCT GAG GCG CTT CCG GCA GCG A* UAA AAA AAA GAAUUC
copA-S1	N.A.	N.A.	N.A.	GGGACCAGCAGGCGGACCACCGGACCAGGGAAGUCAAAAAUUUAAAA GUUAA AGGGAG AUAUA **AUG** UAU UUU GUU CGU *GAA CCG CTG GCG GAG TCA TCA ATC CCG TCG GAA GCA CTG ACA GCC CTT TCT GAG GCG CTT CCG GCA GCG A* UAA AAA AAA GAAUUC
copA-S2	N.A.	N.A.	N.A.	GGGACCAGCAGGCGGACCACCGGACCAGGGAAGUCAAAAAUUUAAAA GUUAA AGGGAG AUAUA **AUG** UAU UUU GUU CGU *GAA CCG CTG GCG GAG TCA TCA ATC CCG TCG GAA GCA CTG ACA GCG GTT TCT GAG GCG AAA AAA AAA GCG A* UAA AAA AAA GAAUUC

[a] The gray shading sequence is the Shine–Dalgarno (SD) sequence, the bold sequence is the translation starting site initiator fMet. The underlined sequence contains a non-slippery sequence and codes Tyr-Phe-Val-Arg. For mRNAs with a slippery sequence, the underlined sequence is replaced by GUA AAA AAG UUU, which codes Val-Lys-Lys-Phe in 0 frame. The italized sequence is the mRNA secondary structure, whose unfolding free energies and unfolding forces were listed in the Table.

Table S2 mRNA sequence and -1 PRF efficiency of ScYLV and HERV variants

mRNA	mRNA sequences with a common slippery sequence (from 5' to 3') [a]	-1 PRF efficiency measured by single-molecule counting (%) [b]
ScYLV-WT	GGGACCAGCAGGCGGACCACCGGACCAGGGAAGUCAAAAAUUUAAAAGUUAA AGGGAG AUAUA **AUG** GUA AAA AAG UUU *CCA AGT GGC GCC GAC CAC TTA AAA ACA CCG GA* UAA AAA AAA GAAUUC	60±3
ScYLV-UUC CCA	GGGACCAGCAGGCGGACCACCGGACCAGGGAAGUCAAAAAUUUAAAAGUUAA AGGGAG AUAUA **AUG** GUA AAA AAG UUC *CCA AGT GGC GCC GAC CAC TTA AAA ACA CCG GA* UAA AAA AAA GAAUUC	59±2
ScYLV-UUU GCA	GGGACCAGCAGGCGGACCACCGGACCAGGGAAGUCAAAAAUUUAAAAGUUAA AGGGAG AUAUA **AUG** GUA AAA AAG UUU *GCA AGT GGC GCC GAC CAC TTA AAA ACA CCG GA* UAA AAA AAA GAAUUC	58±2
HERV-WT	GGGACCAGCAGGCGGACCACCGGACCAGGGAAGUCAAAAAUUUAAAAGUUAA AGGGAG AUAUA **AUG** GUA AAA AAG UUU *CAA AGG GGC CAG CCU CAG GCC CCA CAA CAA ACU GGG GCA U* UAA AAA AAA GAAUUC	47±1
HERV-UUC CAA	GGGACCAGCAGGCGGACCACCGGACCAGGGAAGUCAAAAAUUUAAAAGUUAA AGGGAG AUAUA **AUG** GUA AAA AAG UUC *CAA AGG GGC CAG CCU CAG GCC CCA CAA CAA ACU GGG GCA U* UAA AAA AAA GAAUUC	45±3
HERV-UUU GAA	GGGACCAGCAGGCGGACCACCGGACCAGGGAAGUCAAAAAUUUAAAAGUUAA AGGGAG AUAUA **AUG** GUA AAA AAG UUU *GAA AGG GGC CAG CCU CAG GCC CCA CAA CAA ACU GGG GCA U* UAA AAA AAA GAAUUC	45±4

[a] The gray shading sequence is the Shine–Dalgarno (SD) sequence, the bold sequence is the translation starting site initiator fMet. The underlined sequence contains a slippery sequence and codes Val-Lys-Lys-Phe in 0 frame. The italized sequence is the mRNA secondary structure.

[b] –1 PRF efficiency was measured by single-molecule counting in the presence of the slippery sequence (A AAA AAG) and calculated from three independent replicates.

Table S3 -1 PRF efficiency and dwell time of ribosomal complexes during ongoing elongation experiments with copA and its mutant variants

mRNA structure	-1 PRF efficiency (%) [a]	Dwell time in the first pseudoknot-unwinding cycle			
		non-slippery sequence		slippery sequence	
		PRE^{FV} (s)	$POST^{FV}$ (s)	PRE^{K1K2} (s)	$POST^{K1K2}$ (s)
copA-WT	30±3	0.9±0.2	5.1±0.6	2.7±0.1	3.6±0.4
copA-S1	7±2	1.1±0.1	2.5±0.4	2.3±0.1	1.5±0.4
copA-S2	21±2	1.0±0.2	3.8±0.2	2.9±0.2	2.4±0.3

SEMs were calculated from three independent replicates.

[a] –1 PRF efficiency was measured by single-molecule counting in the presence of the slippery sequence (A AAA AAG) and calculated from three independent replicates.

Table S4 Dwell time of non-ratcheted and ratcheted ribosomal complexes containing the non-slippery sequence during stalled experiments

mRNA structure	Dwell time in the first cycle				Dwell time in the second cycle			
	Non-ratcheted $POST^{F}$ (s)	Ratcheted $POST^{F}$ (s)	Non-ratcheted PRE^{FV} (s)	Ratcheted PRE^{FV} (s)	Non-ratcheted $POST^{V}$ (s)	Ratcheted $POST^{V}$ (s)	Non-ratcheted PRE^{VR} (s)	Ratcheted PRE^{VR} (s)
PL	0.49±0.04	1.06±0.14	0.53±0.03	1.30±0.09	0.43±0.03	0.38±0.02	0.38±0.01	0.39±0.01
PT2G32	0.38±0.03	1.12±0.11	0.44±0.03	1.21±0.08	0.36±0.03	0.40±0.02	0.34±0.03	0.48±0.04
PEMV1	0.35±0.06	1.26±0.01	0.38±0.06	1.13±0.01	0.40±0.04	0.46±0.03	0.42±0.02	0.46±0.02
ScYLV	0.29±0.01	1.71±0.01	0.28±0.01	0.94±0.02	0.46±0.02	0.47±0.02	0.43±0.02	0.48±0.02
HERV	0.32±0.05	1.41±0.13	0.37±0.02	1.09±0.11	0.45±0.07	0.56±0.05	0.42±0.06	0.56±0.07
VMV	0.29±0.01	1.53±0.10	0.34±0.07	1.10±0.02	0.43±0.04	0.46±0.03	0.39±0.02	0.42±0.01
Pearson correlation coefficient [a]	-0.89* (0.02)	0.98* (0.01)	-0.95* (0.01)	-0.97* (0.01)	0.67 (0.15)	0.72 (0.11)	0.72 (0.11)	0.46 (0.35)

Mean±SEM was calculated from three or more independent replicates.

[a] Pearson correlation coefficient between dwell times of each ribosomal complex and -1 PRF efficiency measured by single-molecule counting. Corresponding p-value was listed within parentheses. * indicated significant correlation.

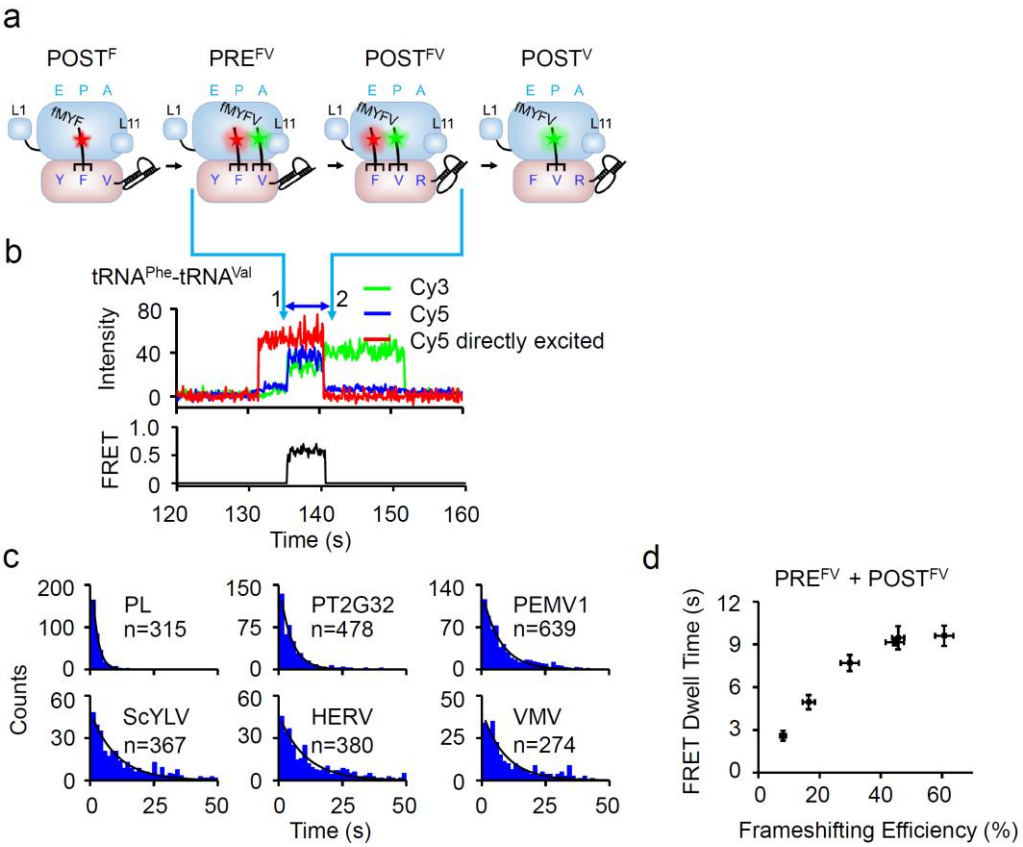

Fig. S1. Elongation rates of ribosomes on non-slippery mRNAs measured using Cy5-tRNA^{Phe}/Cy3-tRNA^{Val} FRET pair during the first pseudoknot-unwinding cycle. a) Schematic drawings of ribosomal complexes from POST^{F} to POST^{V}. b) Typical real-time trace measured using Cy5-tRNA^{Phe}/Cy3-tRNA^{Val} FRET pair for ribosomes programmed with mRNAs containing the non-slippery sequence. In addition to Cy3 fluorescence (green) and Cy5 fluorescence (FRET, blue) under 532 nm excitation, Cy5 direct fluorescence (red) was also collected under alternating 640 nm laser excitation. Accommodation of Cy3-tRNA^{Val} into the A-site led to spontaneous appearance of Cy3 and FRET signals (arrow 1). Dissociation of Cy5-tRNA^{Phe} from the E-site caused spontaneous disappearance of Cy5 and FRET signals (arrow 2). Dwell time of FRET state between arrows 1 and 2 corresponded to the total dwell times of PRE^{FV} and POST^{FV} complexes. c) Dwell time distributions of the Cy5-tRNA^{Phe}/Cy3-tRNA^{Val} FRET state with different pseudoknots. d) Plot of FRET dwell time versus frameshifting efficiency. n is the number of events. Dwell times were extracted by single exponential fitting of dwell time distributions. Error bars were standard errors.

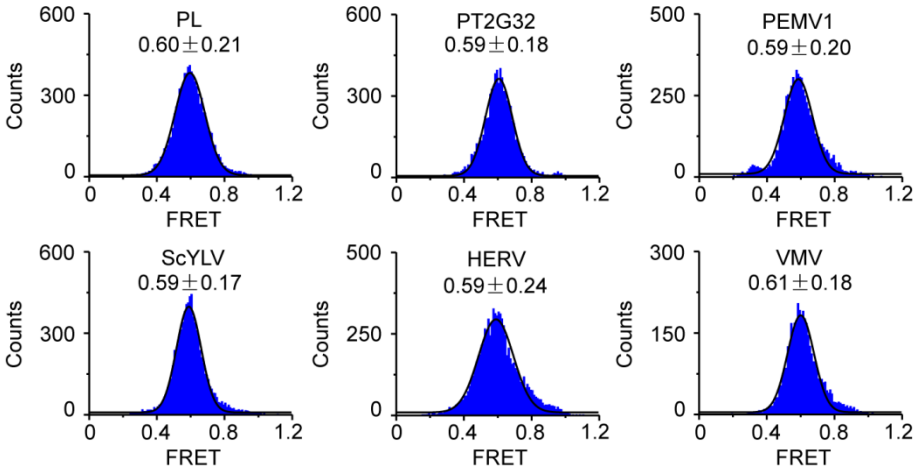

Fig. S2. FRET distributions between Cy3-tRNA^{Val} and Cy5-L11 during on-going elongation. Distributions were accumulated from FRET values of each frame before translocation. Fitting to Gaussian distribution showed one major peak at ~0.6 for all mRNA constructs. Mean±SD was indicated.

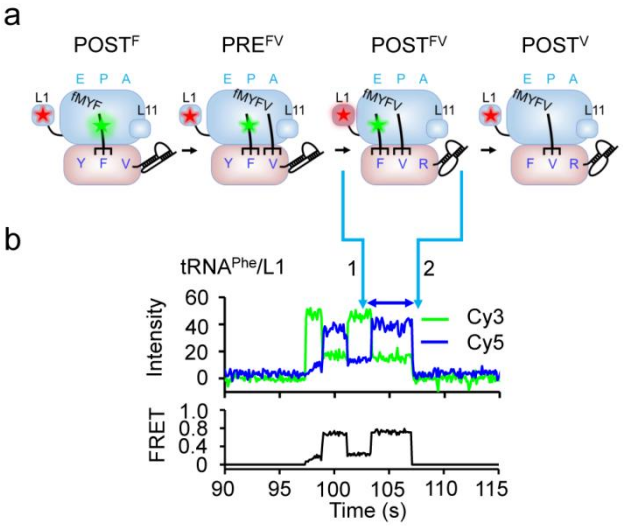

Fig. S3. Dwell time of POST^{FV} complex during ongoing translation captured by Cy3-tRNA^{Phe}/Cy5-L1 FRET. a) Schematic drawings of ribosomal complexes from POST^{F} to POST^{V}. b) Typical real-time trace measured using Cy3-tRNA^{Phe}/Cy5-L1 FRET pair for ribosomes programmed with mRNAs containing the non-slippery sequence. Arriving of Cy3-tRNA^{Phe} into the E-site led to formation of the high FRET state (arrow 1). Dissociation of Cy3-tRNA^{Phe} from the E-site caused spontaneous disappearance of Cy3 and FRET signals (arrow 2). The last high FRET state between arrows 1 and 2 corresponded to POST^{FV} complex.

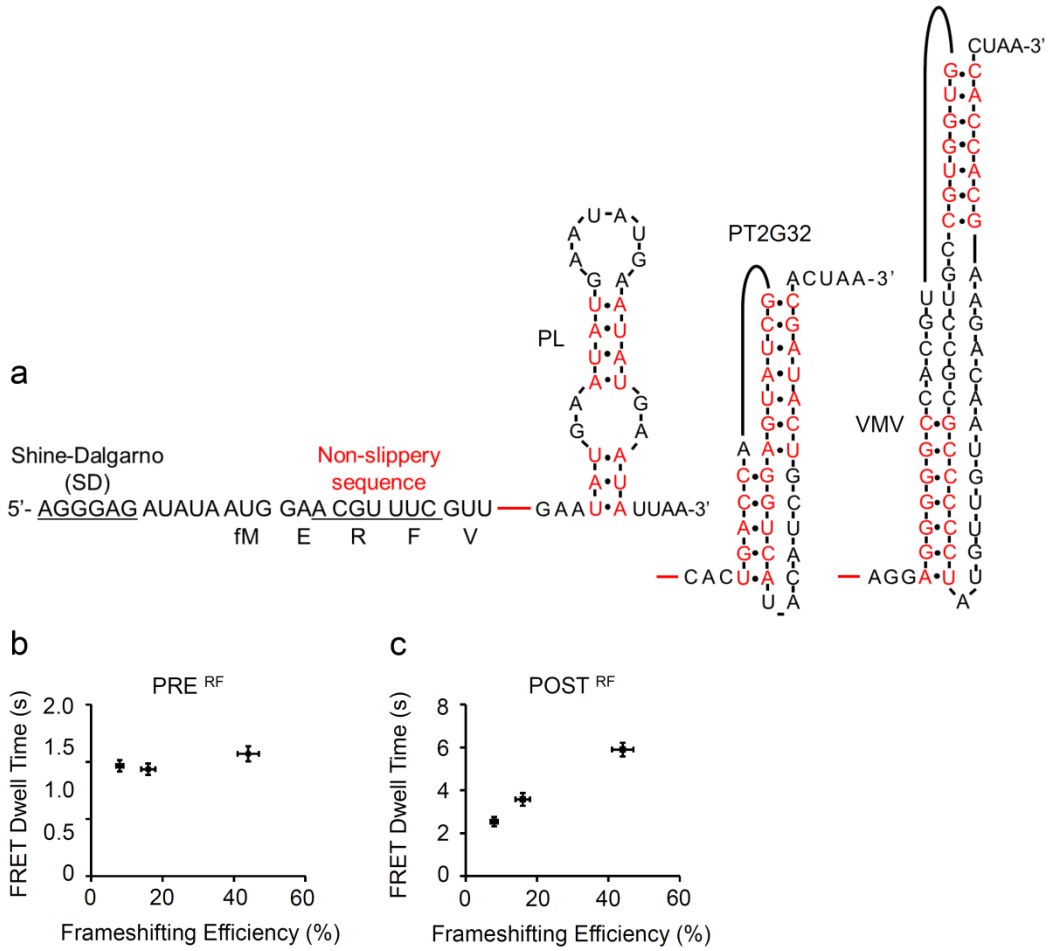

Figure S4. Elongation rates of ribosomes on non-slippery mRNAs (fMERFV) with different pseudoknots sequence during the first pseudoknot-unwinding cycle. a) mRNA constructs and their secondary structures. mRNA contained a common non-slippery sequence (fMERFV) was used. fM, E, R, F and V are abbreviations for initiator Methionine, Glutamic acid, Arginine, Phenylalanine, and Valine, respectively. The Shine-Dalgarno (SD) sequence, non-slippery sequence (A CGU UUC) was underlined. Pseudoknots PT2G32 and VMV were placed downstream from the common mRNA sequences. An unstable secondary structure PL was used as a control. b) Plot of PRE^{RF} dwell time versus frameshifting efficiency. c) Plot of $POST^{RF}$ dwell time versus frameshifting efficiency. Error bars were standard errors.

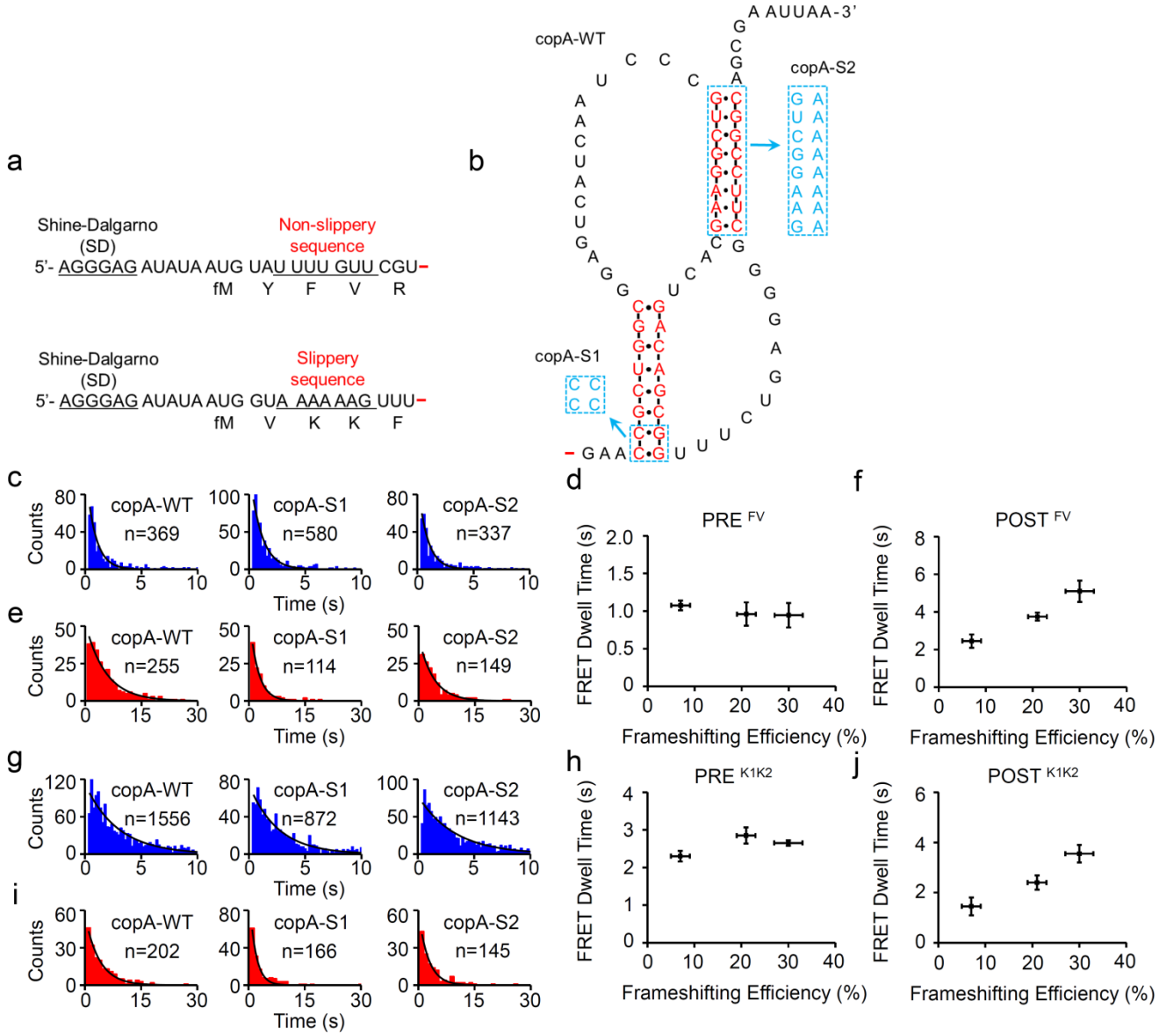

Figure S5. Elongation rates of ribosomes on mRNAs with copA and its mutant variants during the first pseudoknot-unwinding cycle. a and b) mRNA constructs and their secondary structures. Two sets of mRNAs were used. One set contained a common non-slippery sequence (fMYFVR) and the other had a common slippery sequence (fMVKKF). fM, Y, F, V, R, and K are abbreviations for initiator Methionine, Tyrosine, Phenylalanine, Valine, Arginine, and Lysine, respectively. The Shine-Dalgarno (SD) sequence, non-slippery sequence (U UUU GUU), and slippery sequence (A AAA AAG) were underlined. Pseudoknots copA-WT, copA-S1, and copA-S2 were placed downstream from the common mRNA sequences. Their full sequences were shown in Table S1. Base pairs within secondary structures were indicated in red, whereas unpaired bases were indicated in black. Boxes and arrows indicate the mutations. c) Dwell time distributions of PRE^{FV} complexes captured during ongoing elongation. d) Plot of PRE^{FV} dwell time versus frameshifting efficiency. e) Dwell time distributions of $POST^{FV}$ complexes during ongoing elongation. f) Plot of $POST^{FV}$ dwell time versus frameshifting efficiency. g) Dwell time distributions of PRE^{K1K2} complexes captured during ongoing elongation. h) Plot of PRE^{K1K2} dwell time versus frameshifting efficiency. i) Dwell time distributions of $POST^{K1K2}$ complexes during ongoing elongation. j) Plot of $POST^{K1K2}$ dwell time versus frameshifting efficiency. n is the number of events. Dwell times were extracted by single exponential fitting of dwell time distributions. Error bars were standard errors.

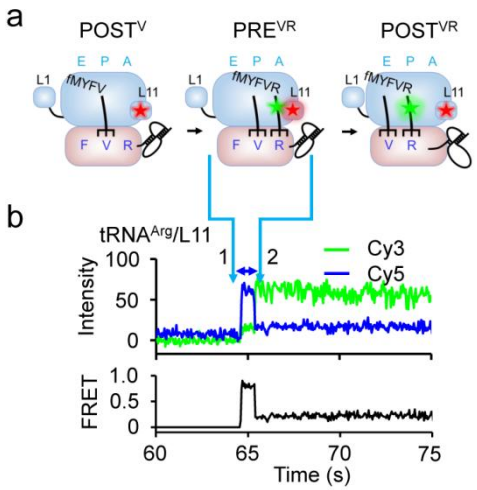

Fig. S6. Dwell time of PRE^{VR} complex during ongoing translation captured by Cy3-$tRNA^{Arg}$/Cy5-L11 FRET. a) Schematic drawings of ribosomal complexes from $POST^{V}$ to $POST^{VR}$. b) Typical real-time trace measured using Cy3-$tRNA^{Arg}$/Cy5-L11 FRET pair. Accommodation of Cy3-$tRNA^{Arg}$ into the A-site led to spontaneous appearance of Cy3 and FRET signals (arrow 1). Translocation from PRE^{VR} to $POST^{VR}$ caused decrease of FRET accompanied by increase of Cy3 signals (arrow 2). The high FRET state between arrows 1 and 2 corresponded to PRE^{VR} complex.

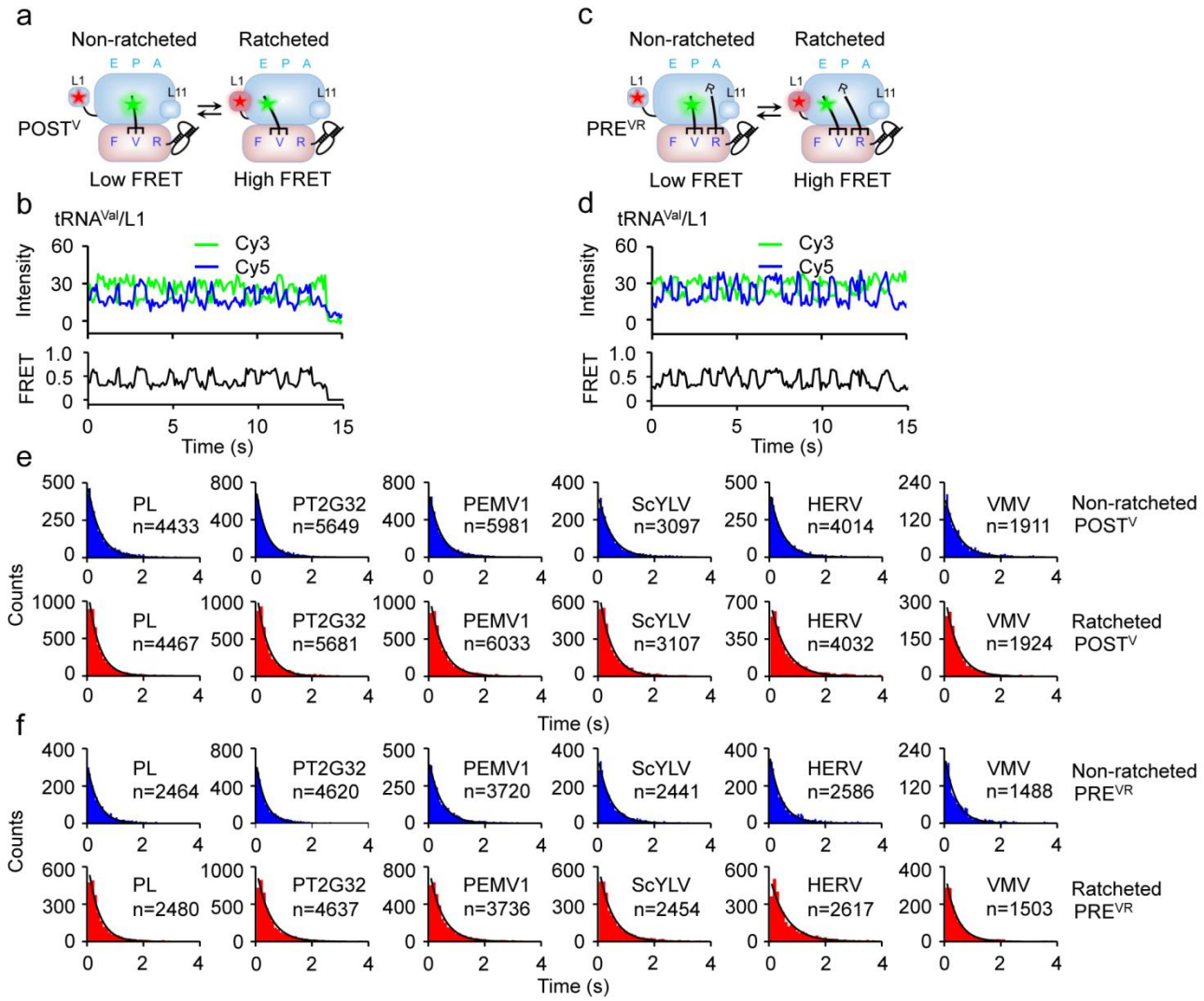

Fig. S7. Conformational dynamics of stalled ribosomal complexes on non-slippery mRNAs in the secondary pseudoknot-unwinding cycle. a-d) Schematic drawings (a and c) and example traces (b and d) using Cy3-tRNA^{Val}/Cy5-L1 FRET pair to capture conformational dynamics of POST^{V} (a and b) and PRE^{VR} (c and d) complexes. In both POST^{V} and PRE^{VR} complexes, ribosomes spontaneously transit between the non-ratcheted (low FRET) and ratcheted (high FRET) states, which were captured by smFRET as shown in b and d. e) Dwell time distributions of the non-ratcheted and ratcheted POST^{V} states with different pseudoknots. f) Dwell time distributions of the non-ratcheted and ratcheted PRE^{VR} states with different pseudoknots. 5 mM puromycin was applied to POST^{V} complexes for 5 min to remove nascent peptides before smFRET recording. PRE^{VR} were formed by incubating puromycin-treated POST^{V} with Arg-tRNA^{Arg} ternary complex. n is the number of events.

Reference

1. Chen, C.L., Zhang, H.B., Broitman, S.L., Reiche, M., Farrell, I., Cooperman, B.S. and Goldman, Y.E. (2013) Dynamics of translation by single ribosomes through mRNA secondary structures. *Nature Structural & Molecular Biology*, **20**, 582-588.
2. Neupane, K., Ritchie, D.B., Yu, H., Foster, D.A., Wang, F. and Woodside, M.T. (2012) Transition path times for nucleic Acid folding determined from energy-landscape analysis of single-molecule trajectories. *Phys Rev Lett*, **109**, 068102.
3. Wang, Y., Wills, N.M., Du, Z., Rangan, A., Atkins, J.F., Gesteland, R.F. and Hoffman, D.W. (2002) Comparative studies of frameshifting and nonframeshifting RNA pseudoknots: a mutational and NMR investigation of pseudoknots derived from the bacteriophage T2 gene 32 mRNA and the retroviral gag-pro frameshift site. *RNA (New York, N.Y.)*, **8**, 981-996.
4. Nixon, P.L., Rangan, A., Kim, Y.G., Rich, A., Hoffman, D.W., Hennig, M. and Giedroc, D.P. (2002) Solution structure of a luteoviral P1-P2 frameshifting mRNA pseudoknot. *Journal of molecular biology*, **322**, 621-633.
5. Cornish, P.V., Hennig, M. and Giedroc, D.P. (2005) A loop 2 cytidine-stem 1 minor groove interaction as a positive determinant for pseudoknot-stimulated -1 ribosomal frameshifting. *Proceedings of the National Academy of Sciences of the United States of America*, **102**, 12694-12699.
6. Pennell, S., Manktelow, E., Flatt, A., Kelly, G., Smerdon, S.J. and Brierley, I. (2008) The stimulatory RNA of the Visna-Maedi retrovirus ribosomal frameshifting signal is an unusual pseudoknot with an interstem element. *RNA (New York, N.Y.)*, **14**, 1366-1377.